Proceedings of ASME Turbo Expo 2018: Turbomachinery Technical Conference and Exposition
GT2018
June 12-14, 2018, Oslo, Norway

GT2018-75790

HYDRODYNAMIC JOURNAL BEARINGS OPTIMIZATION CONSIDERING ROTOR DYNAMICS RESTRICTIONS

Dr. Leonid Moroz
SoftInWay Inc.
1500 District Ave, Burlington, MA 01803, USA
L.Moroz@softinway.com

Dr. Leonid Romanenko
SoftInWay Inc.
1500 District Ave, Burlington, MA 01803, USA
L.Romanenko@softinway.com

Dr. Roman Kochurov
SoftInWay Inc.
1500 District Ave, Burlington, MA 01803, USA
R.Kochurov@softinway.com

Evgen Kashtanov
SoftInWay Inc.
1500 District Ave, Burlington, MA 01803, USA
E.Kashtanov@softinway.com

ABSTRACT

In this study, optimal designs of hydrodynamic journal bearings for 13.5 MW induction motor prototype is developed based on the design of experiment approach and best sequences method which involves entire rotor-bearing system multidisciplinary simulations. These simulations consist of bearing hydrodynamic characteristics calculation and optimization and rotor dynamics analyses for a rotor-bearing system. The results of rotor dynamics analyses are taken into account as the constraints during optimization.

Several journal bearings such as plain cylindrical with a different configuration of pockets, elliptical type, and 4-lobe fixed pad have been considered to select the most appropriate design for the application. The bearing clearance, length, diameter, pockets positions, lobe width, oil viscosity, are applied as design input variables. To find the bearing optimal design, following objective functions were considered:

1) Minimum oil film thickness. Optimal bearing clearance is designed to produce the maximum possible level of minimum oil film thickness in order to avoid or reduce possible metal-to-metal contact;
2) Maximization of the performance is done by minimization of friction power loss.
3) Rotor dynamics simulation for the rotor-bearing system is embedded in the optimization process in order to avoid resonances by providing sufficient critical speeds separation margins from operating speed.

The methodology for the bearing simulation is based on the mass-conserving mathematical model, proposed by Elrod & Adams and numerical solution for the equations is generated using finite difference method. Rotor dynamics analyses are performed using finite element method.

As the result of the study, optimized bearing designs for 13.5 MW induction motor were generated. Optimized bearings provide sufficient frequency margins for critical speeds for the rotor-bearing system and, at the same time, improved hydrodynamic bearing characteristics: maximized oil film thickness and increased efficiency compared to the starting design.

Through the considered bearings examples, the study shows how different parameters, such as bearing clearance, length, diameter, and etc., influence key performance characteristics like bearing minimum oil film thickness, friction power losses, rotor-bearing system critical speeds.

NOMENCLATURE

AF – amplification factor
BSM – best sequences method
CS – critical speed
DOE – design of experiment
DE – drive end
FDM – finite difference method
FEM – finite element method
MOFT – minimal oil film thickness
NDE – non-drive end

INTRODUCTION

High-performance rotating machines usually operate at a high rotational speed and produce significant static and dynamic loads that act on the bearings. Fluid film journal bearings play a significant role in machine overall reliability and rotor-bearing

system vibration and performance characteristics. The increase of bearings complexity along with their applications severity make it challenging for the engineers to develop a reliable design. Bearing modeling should be based on accurate physical effects simulation. To ensure bearing reliable operation, the design should be performed based not only on simulation results for the hydrodynamic bearing itself but also, taking into the account rotor dynamics results for the particular rotor-bearing system, because bearing characteristics significantly influence the rotor vibration response.

Numbers of scientists and engineers have been involved in a journal bearing optimal design generation. A brief review of works dedicated to various aspects of bearing optimization is presented in [1]. Based on the review it can be concluded, that the performance of isolated hydrodynamic bearing can be optimized by proper selection of the length, clearance, and lubricant viscosity. Another conclusion is that the genetic algorithms and particle swarm optimization can be successfully applied to optimize the bearing design. Journal bearings optimizations based on genetic algorithms are also considered in [2-5]. The studies show the effectiveness of the genetic algorithms. At the same time, the disadvantages of the approach are high complexity and a greater number of function evaluations in comparison with numerical methods, which require significantly higher computational efforts and time for the optimization. A numerical evolutionary strategy and an experimental optimization on a lab test rig were applied to get the optimal design of a tilting pad journal bearing for an integrally geared compressor in [6]. The final result of numerical and experimental optimizations was tested in the field and showed that the bearing pad temperature could be significantly decreased. Optimal journal bearing design selection procedure for a large turbocharger is described in [7]. In this study power loss, rotor dynamics instability, manufacturing, and economic restrictions are analyzed. To optimize the oil film thickness by satisfying the condition of maximizing the pressure in a three-lobe bearing, the multi-objective genetic algorithm was used in [8]. In the reviewed studies the optimization has been performed for 'isolated' bearing and influence on rotor dynamics response was not considered.

For higher reliability and longer life of rotating mechanical equipment, the vibration of the rotor-bearing system and of the entire drive train should be as low as possible. A good practice for safe rotor design typically involves the avoidance of any resonance situation at operating speeds with some margins. One common method of designing low vibration equipment is to have a separation margin between the critical natural frequencies and operating speed, as required by API standard [9]. The bearing design and parameters significantly influence rotor-bearing system critical speeds. Thus, to guarantee low rotor vibrations, the critical speeds separation margins should be ensured at rotor-bearing system design/optimization stage.

Conjugated optimization for the entire rotor-bearing system is a challenging task due to various conflicting design requirements, which should be fulfilled. In [10] parameters of rotor-bearing systems are optimized simultaneously. The design objective was the minimization of power loss in bearings with constraints on system stability, unbalance sensitivities, and bearing temperatures. Two heuristic optimization algorithms, genetic and particle-swarm optimizations were employed in the automatic design process.

There are several objective functions that are considered by researchers to optimize bearing geometry, such as

- Optimum load carrying capacity [5];
- Minimum oil film thickness and bearing clearance optimization [1, 6, 8];
- Power losses minimization [6, 7];
- Rotor dynamics restrictions;
- Manufacturing, reliability and economics restrictions [7].

The most common design variables which are considered in reviewed works are clearance, bearing length, diameter, oil viscosity, and oil supply pressure.

Finding the minimum power loss or optimal load carrying capacity together with the entire rotor-bearing system dynamics restrictions, require to employ optimization techniques, because accounting the effects from all considered parameters significantly enlarge the analysis process. Several numerical methods, such as FDM and FEM are usually employed to solve this complex problem and calculation process can sometimes be time-consuming and takes a large amount of computing capacity. To leverage this optimization tasks, efficient algorithms are needed.

In the current study, the optimization approach, which is based on DOE and best sequences method (BSM) [11, 12] and allows to generate journal bearings with improved characteristics was developed and applied to 13.5 MW induction motor application. The approach is based on coupled analysis of bearing and entire rotor-bearing system dynamics to satisfy API standard requirements.

1. PROBLEM FORMULATION AND ANALYSIS METHODS DESCRIPTION

The goal of the work is to increase reliability and efficiency for the 13.5 MW induction motor prototype (Fig. 1) by oil hydrodynamic journal bearings optimization.

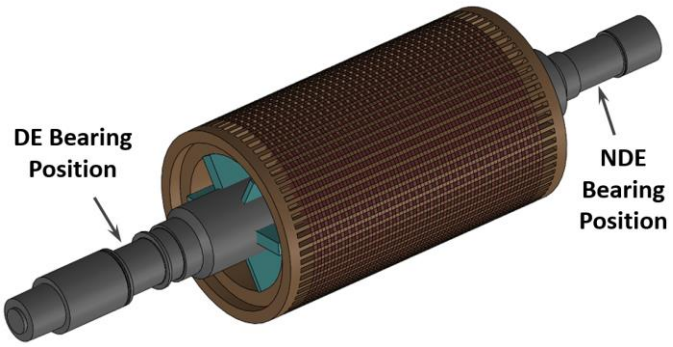

Figure 1: Rotor of 13.5 MW Induction Motor

The motor operating parameters and rotor characteristics are presented below:

Rated speed	rpm	1750
Minimum operating speed	rpm	1750
Maximum operating speed	rpm	1750
Mass of the rotor	kg	6509
Length of the rotor	mm	3500

Initially, for the motor application, plain cylindrical journal bearings were chosen to support the rotor. The scheme of the DE (drive end) and NDE (non-drive end) baseline bearings designs is presented in Fig. 2. For baseline designs, bearing loads were 35 kN for DE and 28 kN for NDE bearing.

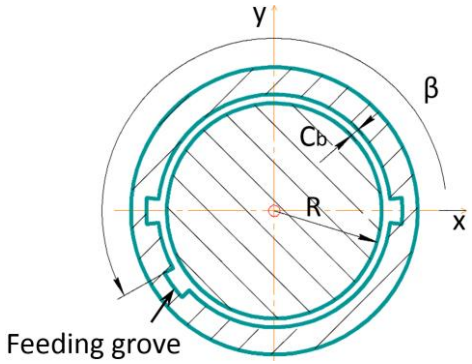

Figure 2: Plain Cylindrical Bearing

The methodology for the bearing characteristics simulation is based on the mass-conserving mathematical model, proposed by Elrod & Adams [13], which is by now well-established as the accurate tool for simulation in hydrodynamic lubrication including cavitation. This model contains two unknown fields, one of which is the pressure p and the other the fluid fraction variable θ, which takes values between zero and one. The governing equation are presented below

$$div(h^3\nabla p) = \alpha\frac{\partial(\theta h)}{\partial x_1} + 2\frac{\partial(\theta h)}{\partial t} \text{ in } \Omega\backslash\Sigma; \quad (1)$$
$$p \geqslant 0,\ \theta = 1 \text{ in } \Omega^+;$$
$$p = 0,\ \theta < 1 \text{ in } \Omega_0;$$
$$p = 0 \text{ on } \Sigma\backslash\Gamma_0$$
$$p = p_a \text{ on } \Gamma_a$$

where

x_1-axis is chosen parallel to the (fixed) sliding velocity;
h – gap thickness function;
Ω – non-dimensional computational domain;
Ω^+ – the pressurized region of the bearing;
Ω_0 – cavitated region
Σ – the internal boundary between Ω^+ and Ω_0 (cavitation boundary)
Γ_0 – outlet boundary;
Γ_a – feeding boundary;
p_a – oil supply pressure,

supplemented with the mass-conservation condition at the cavitation boundary:

$$(h_0\theta_0 - h_+)\,\alpha\,\hat{e_1}\hat{n} + h_+^3\left(\frac{\partial p}{\partial n}\right)_+ = 2(h_0\theta_0 - h_+)V_n, \quad (2)$$

where

α – non-dimensional sliding velocity, assumed parallel to $\hat{e_1}$;
$\hat{e_1}$ – the unit vector parallel to x_1;
$\hat{n}$ is the unit vector normal to Σ, oriented outwards from Ω^+;
V_n represents the local normal velocity at which Σ is moving;

the subscripts 0 and + refer to the limit values of the variables as Σ is approached from the cavitated and active regions, respectively.

The equations and boundary conditions (1) and (2) are solved in time starting from an initial condition

$$\theta(x_1x_2, t = 0) = \theta_0(x_1, x_2) \quad (3)$$

The Elrod & Adams model is expanded with heat conduction equations. Additional modifications to account turbulent flow regime and compressible fluid were incorporated in the solver. The numerical solution of the Elrod & Adams equations is generated using finite difference method with successive over-relaxation (SOR) algorithm.

The baseline bearings initial data and calculated hydrodynamical parameters are listed in table 1 (see Fig. 2).

Table 1: Parameters for the Initial Bearing Design

Parameter	Symbol	Units	DE	NDE
Bearing Length	L	m	0.12	0.12
Shaft Diameter	D	m	0.2	0.2
Clearance (radial)	C_b	μm	200	200
Pocket position	β	deg	205	205
Pocket width	dβ	deg	15	15
Oil Grade	-	-	ISO VG 32	
Min oil film thickness	H_{min}	μm	34	38
Friction Power Losses	Nfr	W	2200	2050
Friction coefficient	Fr	-	0.0034	0.0039
Maximum oil pressure	P_{max}	MPa	6.2	4.8

A good practice for safe rotor design typically involves the avoidance of any resonance situation at operating speeds with some margins including resonances by a reason of structural supports vibration. If there is no possibility to change the design to satisfy frequency margins, the vibration amplitudes and forces acting on the bearings have to be measured and analyzed according to standards or company design practice [9].

API 684 standard paragraphs define a critical speed as any rotor-bearing system resonance with amplification factor (AF) greater than 2.5. According to API, AF is a measure of a rotor-bearing system's vibration sensitivity to unbalance when operating in the vicinity of one of its lateral critical speeds. If the AF is less than 2.5, the response is considered critically damped and no separation margin is required. If the AF is higher than 2.5 a separation margin is required. AF can be defined as:

$$AF = \frac{N_{C1}}{N_2 - N_1}, \quad (4)$$

where

N_{C1} – rotor first critical speed, center frequency, cycles per minute;

N_1 – initial (lesser) speed at 0.707 x peak amplitude (critical);

N_2 – final (greater) speed at 0.707 x peak amplitude (critical).

The main body of API 541 [14] does not differentiate between a highly damped resonance and critical speed. As such, no method of calculating the amplification factor or separation margin is made. At the same time, alternate criteria for defining a well-damped resonance [14] which are based on the API some standard paragraphs consider modes of vibration with AFs below 2.5 to be critically damped. These modes are not considered critical speeds because they do not result in high levels of rotor vibration.

The API [14, 15] standards, which can be utilized for the considered case, specifies that lateral critical speeds shall be removed from the operating speed frequency and any other significant excitation frequency by at least 15%, which corresponds to criticals below 1487 rpm and above 2013 rpm for the induction motor application.

To check the possibility of operation near resonance, rotor dynamics analyses have been performed for the baseline rotor-bearing system. The shaft is modeled by Timoshenko beam elements with mass and stiffness properties. The rotor core pack is modeled by means of lumped mass-inertia elements. The rotor dynamics analyses have been performed using finite element method. The FE model for the analysis is presented in Fig. 3.

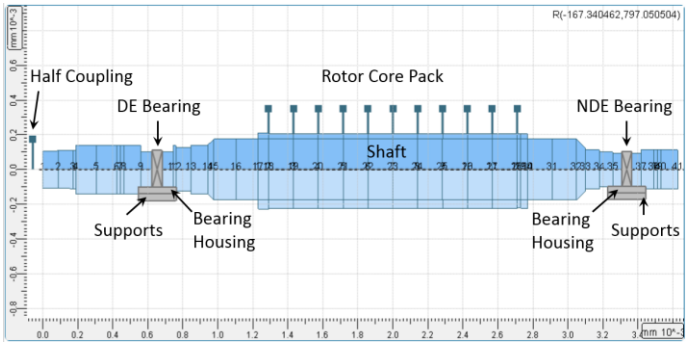

Figure 3: **Rotor Dynamics FE model**

Bearing housing and supports characteristics play a very important role when calculating rotor-bearing system critical speeds and unbalance response. Lack of bearing supports stiffness or bearing supports resonance is one of the major sources of high vibration problems. API 684 [9] states that if the bearing support stiffness is 3.5 times greater than the bearing stiffness in the same direction, the effect of bearing support will be negligible and might not be considered. However, the consideration of support stiffness is recommended by many researches in all cases as it will improve the accuracy of the results [16].

To account the effect of bearing housings and supports, classical model, which assumes series of spring-mass elements, is used. The simulation model is presented in Fig. 3 and equivalent stiffness and mass characteristics for the supports are presented in table 2. Damping and the cross-coupled coefficients in the supports structure were neglected because of the small effect on the results and uncertainty in this properties determination.

Table 2: Bearing Housings and Supports Characteristics

Parameter	Mass	Horizontal Stiffness	Vertical Stiffness
	M, kg	K_{xx}, MN/m	K_{yy}, MN/m
DE Bearing Housing	425	2600	3250
NDE Bearing Housing	230	1650	2150
DE Supports	8700	750	1450
NDE Supports	8700	850	1600

Calculated critical speeds within the range between 0 and motor trip speed for the rotor-bearing system are 1588 rpm, 2376 rpm, and 2733 rpm. Unbalance response analysis for the system shows that first critical speed has insufficient separation margin – less than 8% (see Fig. 4). Calculated AFs for the first critical speed are above 2.5. Baseline rotor-bearing system design demonstrates operation near resonance point, which may cause high vibrations.

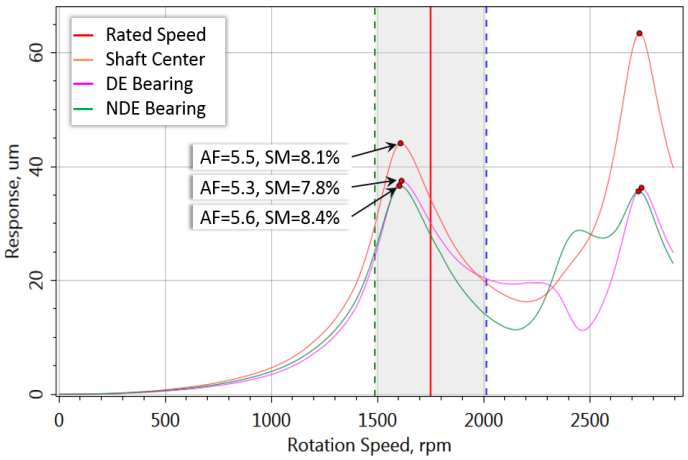

Figure 4: Frequency response characteristics for Baseline Rotor-Bearing System

To overcome baseline design vibration and reliability challenges, the motor rotor-bearing system may be optimized for minimum vibration by avoiding resonances. Another purpose of optimization is to increase efficiency and reliability of bearings for the application. To solve these tasks, it was decided to optimize bearing designs by varying geometrical parameters and changing rotor diameter/length at bearings positions in some narrow range to incorporate new bearings and keep rotor without major changes.

2. BEARINGS OPTIMIZATION PROCEDURE

Three types of bearings were considered in the study. Besides the initial plain cylindrical bearing design (Fig. 2), elliptical (Fig. 5a) and 4-lobe fixed pad (symmetric taper) (Fig. 5b) bearings were optimized to choose the best solution for the application. For elliptical and 4 lobe fixed pad bearings, 0.306 preload and 0.5 offset (determined according to API [9]) were applied.

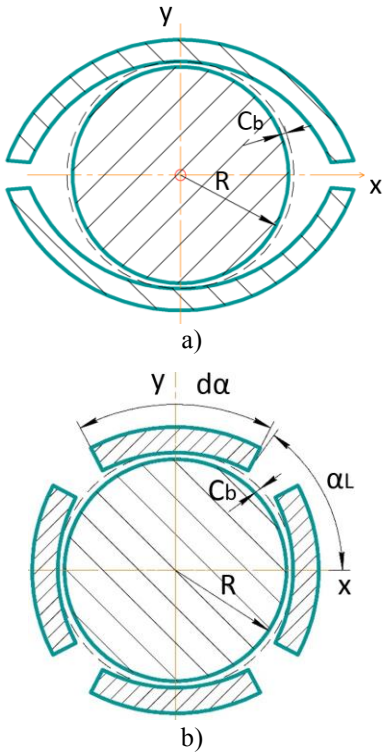

Figure 5: Bearing Schemes: (a) Elliptical; (b) 4-lobe Fixed Pad

The purposes of optimization are to increase reliability and efficiency of the rotor-bearing system. The following objective functions and constraints have been considered for this task:

1) ***Minimal oil film thickness*** (MOFT) is the most critical parameter which influences on the bearing reliability. When its value drops below either the journal surface roughness or the value of the geometric distortions, the hydrodynamic lubrication changes to a mixed lubrication regime, which is characterized by metal-to-metal contact. In order to prevent undesirable metal-to-metal contact, the clearance should be designed to produce the maximum possible level of MOFT;
2) ***Power loss*** minimization leads to machine efficiency increase. To provide minimum level of bearing power loss, the bearing oil film friction coefficient should be as low as possible;
3) ***Lateral critical speeds*** for the rotor-bearing system have to satisfy separation margins. Changing bearing design parameters during optimization results in different bearings mechanical characteristics and consequently deviation in rotor-bearing system critical speeds. Constraints with regards to the critical speeds should be imposed to avoid potential vibration problems.

To perform this multidisciplinary optimization several software modules: DOE optimization, bearing simulation, and rotor dynamics analysis were combined within a supervisor program which manages data exchange and leads optimization process. The principal algorithm for optimization is shown in Fig. 6.

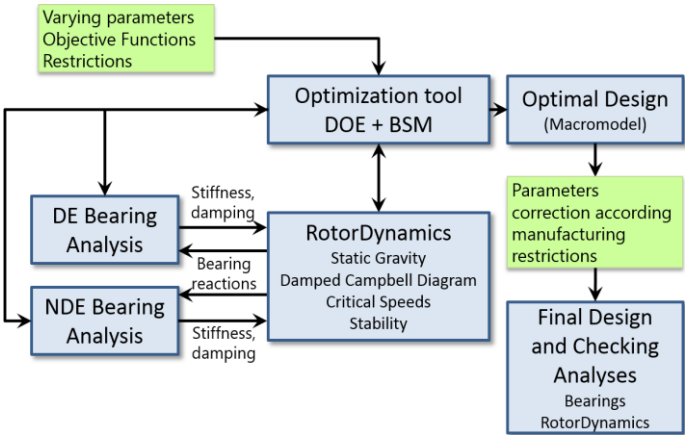

Figure 6: Optimization Algorithm within Supervisor Program

'Optimization tool' in Fig. 6 has embedded subsystem of optimization that allows to create sets of criteria and constraints from among response functions and set up the ranges of variation of independent variables and a search strategy as well. A search of an extremum of intractable yet reasonably smooth functions is expedient using a mechanism of the design of experiment (DOE) theory. An original function is replaced by its 'macro model' extracted from numerical experiment results obtained by computation of the function's values by certain manner selected points.

At the first step of the work, the design of numerical experiment was performed in order to determine the relationship between physical parameters of the rotor-bearing system. Box-Benken approximation plan [11] have been created and used for numerical experiment with the different number of independent variables and computational points for each bearing type:

1) Plain cylindrical bearing – 9 variables and 121 computational points;
2) Elliptical bearing – 7 variables and 49 computational points;
3) 4-lobe Fixed Pad bearing – 7 variables and 49 computational points.

For all bearing designs, radial clearance (C_b), bearing length (L), shaft radius (R) at bearing positions, oil viscosity and additionally, pocket position (β) for plain cylindrical bearings and lobe width ($d\alpha$) for 4 lobe fixed pad design have been varied in some range to find optimal design – see table 3.

Table 3: Variable Parameters Ranges

Parameter	Symb.	Units	Min	Max
Bearing Length	L	m	0.12	0.19
Shaft Diameter	D	m	0.2	0.24
Clearance (radial)	C_b	μm	100	300
Oil viscosity	μ	$N{\cdot}s/m^2$	0.012	0.014
Pocket position (plain cyl.)	β	deg	205	220
Lobe width (4-lobe fix. pad)	dα	deg	70	80

For the points from the approximation plan, the DE and NDE bearings calculation and rotor dynamics analysis were done to fill the plan. Note that bearing length and shaft radius variation influence on shaft mass and stiffness, so change of these parameters in bearing design lead to bearing reactions recalculation and rotor geometry with analysis model correction. The bearing loads were calculated based on corrected rotor geometry for each bearing simulation.

Bearings simulations have been performed based on Elrod & Adams algorithm described above and FDM, utilizing parametrical models shown in Fig. 2 and in Fig. 5. Rotor dynamics FE parametrical model, which was used in optimization process is shown in Fig. 3. Following the procedure presented in Fig. 6, DE and NDE bearings were calculated separately within optimization algorithm and the bearings' characteristics then bearings' mechanical characteristics were exported in RotorDynamics solver. Rotor dynamics simulations were performed in the RotorDynamics solver based on calculated bearings' stiffness and damping characteristics and include damped Campbell diagram analysis to calculate damped critical speeds and check the stability of the system.

The results of computations were transferred back to the optimization module for evaluation of macro models' adequacy, interactive analyses and different kinds of optimization. In case of need, the parameters variation ranges and their interaction were refined, and the process recurred. An example of a calculated plan for the elliptical bearing is presented in the Fig. 7 (objective functions H_{min}, N_{fr} are presented in dimensionless format).

Optimization is conducted with Best Sequences method [12]. This method, likewise the method of direct enumeration, is based on multidimensional regions examination, but versus rectangular grids usage, the LPτ search allows to critically reduce the number of sample points. The method can be used for solving the tasks with several dozens of parameters with minimal requirements to the smoothness of the target function and constraints.

Optimization with macro models assumes searching for a maximum of response functions. A level of influence of the particular response function selected on results of optimization can be defined by weight coefficients assignment. Zero value of weight coefficient means that corresponding response function is imposed with constraints and only those values will be regarded during optimization that will not lead the response function over the limitations imposed. Non-zero values of the weight coefficients are considered in the task of optimization to search for a maximum of linear superposition of the response functions taken with these coefficients. When, for example, searching for minimums, those values are to be negative.

Results of expreriments:

Nur	DDE	LDE	CbDE	DNDE	LNDE	CbNDE	Hmin_DE	Hmin_NDE	NfrDE	NfrNDE	EDE
1	0.24	0.192	0.0002	0.2	0.1425	0.0002	0.73783	0.46102	0.5985	0.3362	0.7308
2	0.24	0.192	0.0002	0.175	0.1425	0.0002	0.73783	0.37378	0.5985	0.2612	0.7308
3	0.24	0.12	0.0002	0.175	0.1425	0.0002	0.41488	0.37378	0.5011	0.2612	0.8498
4	0.2	0.12	0.0002	0.175	0.1425	0.0002	0.32625	0.37378	0.3446	0.2612	0.8826
5	0.2	0.12	0.0002	0.2	0.1425	0.0002	0.32625	0.46102	0.3446	0.3362	0.8826
6	0.2	0.192	0.0002	0.2	0.1425	0.0002	0.56572	0.46102	0.4110	0.3362	0.7934
7	0.24	0.12	0.0002	0.2	0.1425	0.0002	0.41488	0.46102	0.5011	0.3362	0.8498
8	0.2	0.192	0.0002	0.175	0.1425	0.0002	0.56572	0.37378	0.4110	0.2612	0.7934
9	0.22	0.192	0.0003	0.1875	0.16	0.0002	0.56703	0.47876	0.4734	0.3102	0.8673
10	0.22	0.192	0.0003	0.1875	0.125	0.0002	0.56703	0.35806	0.4734	0.2825	0.8673
11	0.22	0.192	0.0001	0.1875	0.125	0.0002	0.70912	0.35806	0.7432	0.2825	0.4925
12	0.22	0.12	0.0001	0.1875	0.125	0.0002	0.42105	0.35806	0.5186	0.2825	0.6910
13	0.22	0.12	0.0001	0.1875	0.16	0.0002	0.42105	0.47876	0.5186	0.3102	0.6910
14	0.22	0.12	0.0003	0.1875	0.16	0.0002	0.32437	0.47876	0.3922	0.3102	0.9240
15	0.22	0.192	0.0001	0.1875	0.16	0.0002	0.70912	0.47876	0.7432	0.3102	0.4925
16	0.22	0.12	0.0003	0.1875	0.125	0.0002	0.32437	0.35806	0.3922	0.2825	0.9240
17	0.22	0.156	0.0003	0.2	0.1425	0.0003	0.44514	0.39463	0.4365	0.3236	0.8962
18	0.22	0.156	0.0003	0.2	0.1425	0.0001	0.44514	0.52635	0.4365	0.4300	0.8962
19	0.22	0.156	0.0003	0.175	0.1425	0.0001	0.44514	0.45609	0.4365	0.3082	0.8962
20	0.22	0.156	0.0001	0.175	0.1425	0.0001	0.5723	0.45609	0.6105	0.3082	0.5826
21	0.22	0.156	0.0001	0.175	0.1425	0.0003	0.5723	0.30839	0.6105	0.2571	0.5826
22	0.22	0.156	0.0001	0.2	0.1425	0.0003	0.5723	0.39463	0.6105	0.3236	0.5826
23	0.22	0.156	0.0003	0.175	0.1425	0.0003	0.44514	0.30839	0.4365	0.2571	0.8962
24	0.22	0.156	0.0001	0.2	0.1425	0.0001	0.5723	0.52635	0.6105	0.4300	0.5826
25	0.24	0.156	0.0002	0.2	0.16	0.0002	0.5755	0.52874	0.5487	0.3513	0.7907

Figure 7: Numerical Experiments Results for Elliptical Bearing

The engineer should make a decision what is more important: higher minimal oil film thickness (MOFT) or lower friction losses and higher efficiency of bearing design and perform optimization according to the requirements. Sometimes, the attainment of one target function contradicts with other target functions optimality.

In this study, three variants of optimal configurations were considered for each bearing type. In the first variant weight coefficients were chosen to optimize both objective functions: maximize minimal oil film thickness and minimize power losses simultaneously, for DE and NDE bearings. The second variant implies optimization with regards to MOFT maximization with high priority. In the third variant, the priority was given to bearing efficiency by minimization of bearing friction power loss – see table 4.

Table 4: Assigned Criteria of Optimality and Constraints

Objective functions	Symbol/ units	Weight coefficients		
		Opt.1	Opt.2	Opt.3
MOFT	H_{min}	1	1	0
Friction power losses	N_{fr}	-1	0	-1
Restrictions		Restrictions		
		Min		Max
1st Critical Speed	CS_1, rpm	0		1487
2nd Critical Speed	CS_2, rpm	2013		4000

3. OPTIMIZATION RESULTS

The results of optimization are presented in tables 5 – 7 for plain cylindrical, elliptical and 4-lobe fixed pad bearings. Optimal solutions calculated with macromodels were simulated in Bearing and RotorDynamics software to confirm the adequacy of the approach. The simulation results are also presented in tables 5 – 7.

Table 5: Plain Cylindrical Bearing Optimization Results

Parameter/objective function and units	Optimal 1		Optimal 2		Optimal 3	
	DE	NDE	DE	NDE	DE	NDE
Bearing length (L), m	0.1917	0.1463	0.1906	0.1559	0.1267	0.1289
Shaft diameter (D), m	0.2086	0.1970	0.2365	0.1955	0.2039	0.1759
Rad. Clearance (C_b), μm	299	278	291	292	255	298
Pocket position (β), deg	206	216	206	211	209	220
Calculated based on Macromodel						
MOFT (H_{min}), μm	56	41	65	43	35	26
Power loss (N_{fr}), W	2642	1901	3350	1955	2185	1461
1st CS, rpm	1475		1477		1467	
2nd CS, rpm	2272		2274		2234	
Calculated in Bearing/RotorDynamics solvers						
MOFT (H_{min}), μm	56	41	65	43	35	26
Power loss (N_{fr}), W	2671	1945	3412	1963	2192	1447
1st CS, rpm	1467		1469		1455	
2nd CS, rpm	2264		2269		2245	

Table 6: Elliptical Bearing Optimization Results

Parameter/objective function and units	Optimal 1		Optimal 2		Optimal 3	
	DE	NDE	DE	NDE	DE	NDE
Bearing length (L), m	0.1908	0.1599	0.1894	0.1538	0.1246	0.1304
Shaft diameter (D), m	0.2313	0.1983	0.2395	0.1982	0.2020	0.1752
Rad. Clearance (C_b), μm	269	173	297	128	220	212
Calculated based on Macromodel						
MOFT (H_{min}), μm	64	55	65	56	34	34
Power loss (N_{fr}), W	3140	2150	3250	2320	2115	1506
1st CS, rpm	1451		1450		1409	
2nd CS, rpm	2338		2445		2185	
Calculated in Bearing/RotorDynamics solvers						
MOFT (H_{min}), μm	64	55	65	56	34	34
Power loss (N_{fr}), W	3156	2136	3323	2310	2121	1508
1st CS, rpm	1460		1453		1466	
2nd CS, rpm	2356		2455		2264	

Table 7: 4-lobe Fixed Pad Bearing Optimization Results

Parameter/objective function and units	Optimal 1		Optimal 2		Optimal 3	
	DE	NDE	DE	NDE	DE	NDE
Bearing length (L), m	0.1542	0.1323	0.1865	0.1597	0.1221	0.1256
Shaft diameter (D), m	0.2003	0.1751	0.2375	0.1993	0.2006	0.1794
Rad. Clearance (C_b), μm	267	180	213	192	249	275
Lobe width (dα), deg	70	70	71	71	70	70
Calculated based on Macromodel						
MOFT (H_{min}), μm	36	30	48	42	28	27
Power loss (N_{fr}), W	2658	1937	5096	2949	2390	1750
1st CS, rpm	1320		1239		1285	
2nd CS, rpm	2043		2077		2056	
Calculated in Bearing/RotorDynamics solvers						
MOFT (H_{min}), μm	35	30	48	42	28	27
Power loss (N_{fr}), W	2678	1927	5111	2930	2412	1775
1st CS, rpm	1359		1238		1332	
2nd CS, rpm	2041		2033		2078	

The comparison between macromodel and Bearing/RotorDynamics software solutions shows good accuracy for all considered designs. The maximal difference does not exceed 3.5%.

Dependence of the response functions and variable parameters can be displayed on charts. Figure 8 shows the change of minimal oil film thickness (Fig. 8a) and friction power loss (Fig. 8b) depending on bearing clearance for DE bearing parameters corresponding optimal 1, optimal 2 and optimal 3 cases. Optimal solutions from tables 5 – 7 are presented by dots (in Fig. 8) for each bearing type.

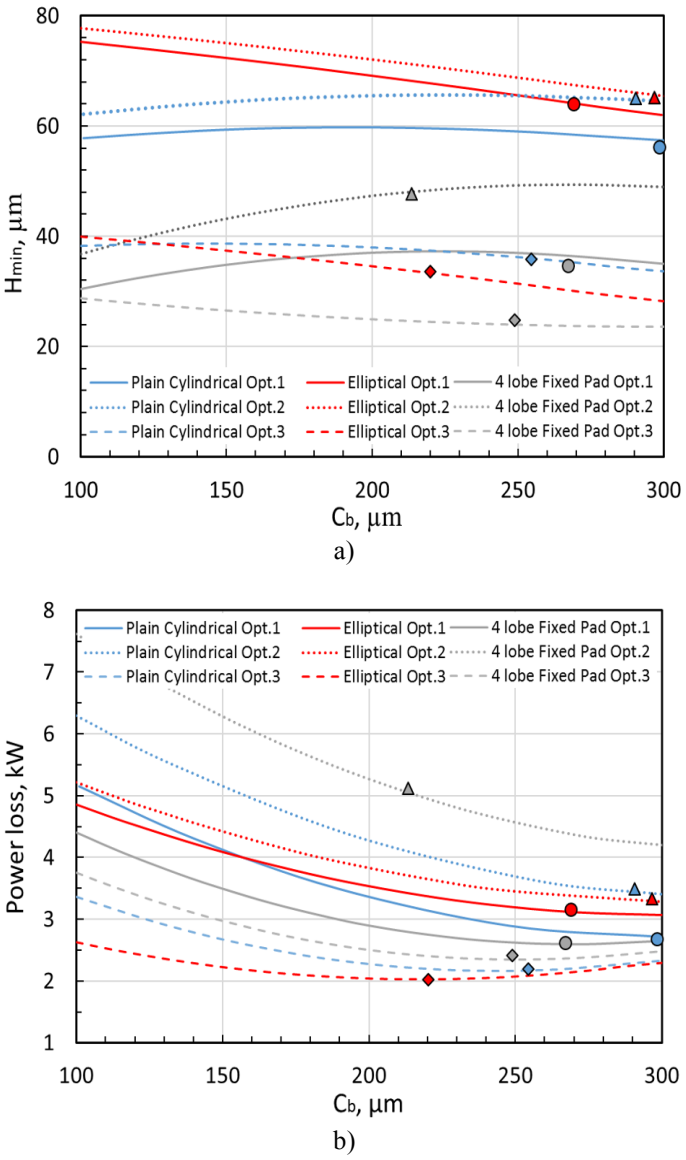

Figure 8: Objective Function vs. Bearing Clearance for DE Bearing: (a) Minimum Oil Film Thickness, (b) Power Loss

Highest MOFT was achieved for elliptical bearing type in optimal 2 case, where MOFT parameter was maximized with high priority. The same elliptical bearing type shows minimal power loss for the optimal 3 case, where power loss was minimized with the highest priority. At the same time, when we consider optimal 3 case, elliptical bearing has sufficient value for the MOFT (>30 μm). Considered 4 lobe fixed pad bearing demonstrates high power loss and lower among other bearings MOFT for all corresponding optimization cases 1 – 3. Optimal 1 case demonstrates middle values for the objective functions for all considered bearing types because in this case both parameters were optimized simultaneously and improvement of one parameter have a negative influence on another.

5. FINAL DESIGN SELECTION

For the final design, preference was given to the bearing with lower friction power loss with acceptable MOFT. Based on optimization results the most suitable option for the application is optimal case #3 for the elliptical bearing type because it provides

1) Lowest bearing friction losses among all other designs;
2) Sufficient minimal oil film thickness which guaranteed no rubbing operation of the bearings;
3) As all calculated optimal solutions, the acceptable separation margins from resonances for the rotor-bearing system is achieved.

According to the scheme in Fig. 6 the last step of the work is to select final parameters for the design with regards to manufacturing restrictions and to perform the scope of checking analyses for the final design. The final parameters for the bearing geometry and simulation results for the optimized elliptical bearing design and comparison with baseline plain cylindrical bearing characteristics are presented in table 8.

Table 8: Baseline and Optimized Bearings Characteristics

Parameter / Objective Function	Symb.	Units	Baseline Plain Cyl.		Optimized Elliptical	
			DE	NDE	DE	NDE
Bearing Length	L	m	0.12	0.12	0.125	0.130
Shaft Diameter	D	m	0.2	0.2	0.202	0.175
Clearance (radial)	C_b	μm	200	200	220	212
Oil grade	-	-	ISO VG 32			
MOFT	H_{min}	μm	34	38	34	34
Power loss	N_{Fr}	W	2201	2042	2116	1520
Max. oil pressure	P_{max}	MPa	6.2	4.8	6.3	5.3
1st Critical Speed	CS_1	rpm	1588		1419	
2nd Critical Speed	CS_2	rpm	2376		2228	
3rd Critical Speed	CS_3	rpm	2733		2670	

Pressure distribution profiles for baseline and optimized designs for DE bearings are presented in the Fig. 9.

DE and NDE final elliptical bearing designs show stable behavior. Bearing stability analysis results are presented in the Fig. 10, where shaft motion trajectory as a result of perturbation is shown in dimensionless coordinates.

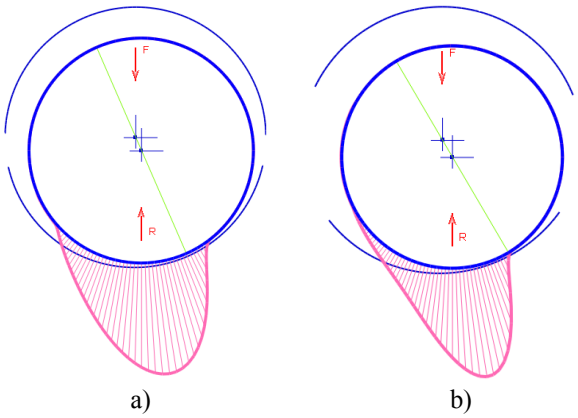

a) b)

Figure 9: Pressure Distribution Profile for DE Bearing: (a) Baseline, (b) Optimized

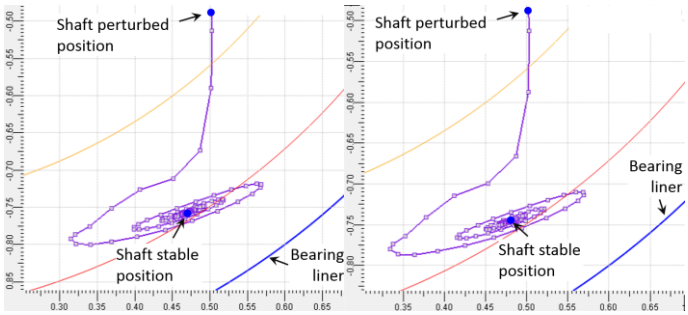

a) b)

Figure 10: Bearing Stability (a) DE, (b) NDE

To confirm reliability and to ensure safe operation for the rotor-bearing system with optimized journal bearings, the full scope of rotor dynamics checking analyses have been performed. A rotor dynamics model for the electric motor was created in the RotorDynamics software and presented in Fig. 3. Bearings map analysis was performed in the Bearing simulation module to calculate bearing mechanical characteristics which are used for rotor dynamics analysis.

Damped Campbell diagram analysis for the rotor-bearing system have been performed and calculated critical speeds for the optimized design are presented in table 8. The results show that optimized rotor-bearing system has following separation margins from minimal/maximal operation speed:

- 18.9% for the 1st critical speed;
- 27.3% for the 2nd critical speed;
- 52.6% for the 3rd critical speed;

which is acceptable according to API Standards [14, 15]. Modal shapes corresponding to the 1st, 2nd and 3rd critical speeds are presented in Fig. 11 and were used to determine the locations for unbalance placement for damped response analysis. It should be noted that first critical speed corresponds to 1st bending rotor mode shape, 2nd critical speed complies with soft supports mode shape and rigid rotor (conical mode), and 3rd CS is a combined rotor-bearing-supports motion.

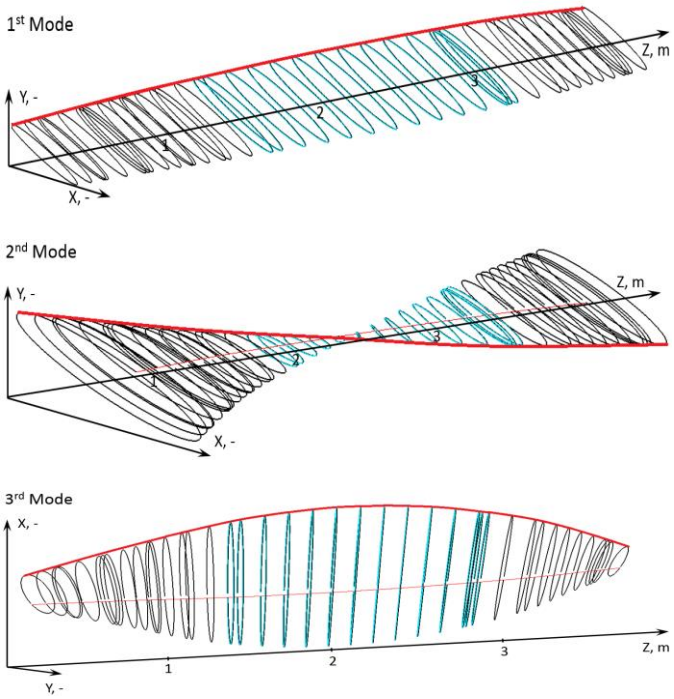

Figure 11: 3D Mode Shapes for the Rotor-Bearing-Supports System

Following [9], unbalances were placed at the rotor center and at rotor ends (see Fig. 12, where red arrows represent unbalances) to excite mode shapes presented in Fig. 11.

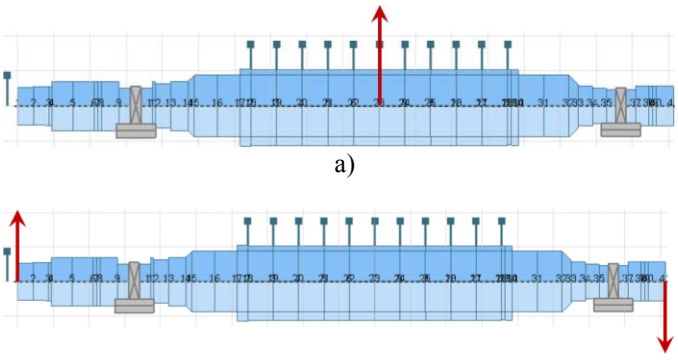

a)

b)

Figure 12: Unbalances to Excite Mode Shapes: (a) Case 1; (b) Case 2

The unbalance values were calculated according to [9] and are equal to 0.23 kg-m for the first unbalance case to excite the mode corresponding to 1st critical speed and 0.13 kg-m for front end force and 0.1 kg-m for rear end force to excite modes corresponding to 2nd critical speed. Frequency response characteristics (maximum major peak-to-peak vibration amplitudes) for the optimized rotor-bearing system are presented in Fig. 13. The response for the initial design is also presented on the graph in Fig. 13 by corresponding lines (see legend on the graphs). Figure 13a represents the unbalance response analysis results for the unbalance case 1. The unbalance case 2 results are presented in Fig. 13b.

The simulation confirms that potential resonances are avoided for the optimized design. In Fig. 13, +/-15% separation margin from operation speed are shown with dashed lines. Actual separation margins for the optimized design calculated based on damped unbalance response analysis are above 17%.

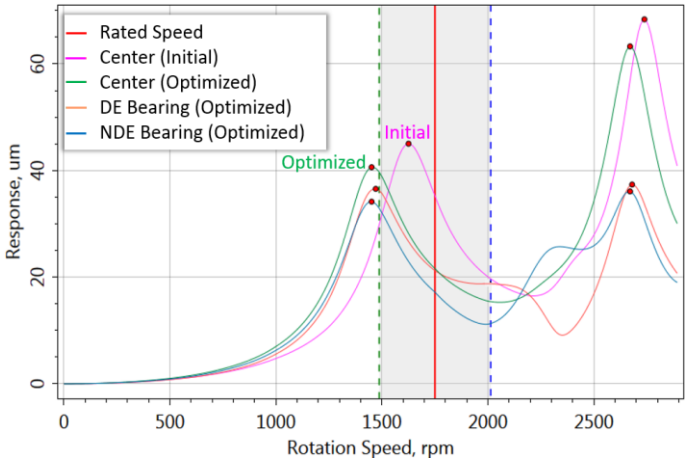

(a)

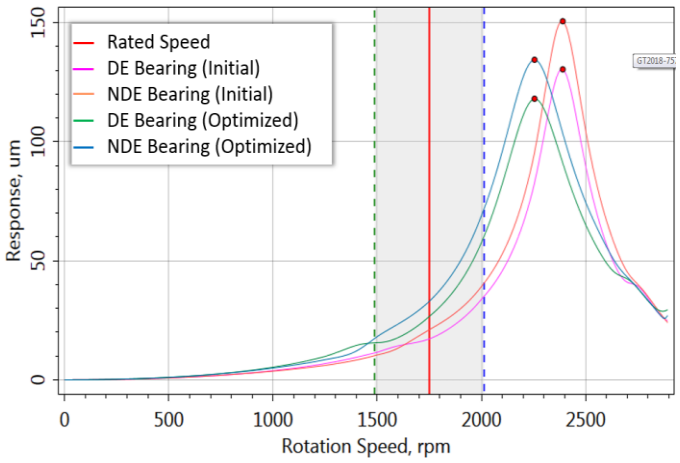

(b)

Figure 13: Frequency response characteristics for the rotor-bearing system. Unbalance applied to excite the mode corresponding to (a) 1st critical speed (b) 2nd critical speed

Table 9 shows the DE and NDE bearing dynamic forces at nominal operating speed and rotor displacements at bearings locations for two unbalance cases for the initial and optimized designs. Absolute displacements from table 9 correspond to the rotor vibration amplitudes relative to the ground. Relative displacements in the table 9 correspond to the differential rotor-to-bearing housing vibration amplitudes. The dynamic forces and displacements analysis results show that vibration forces and amplitudes at bearings location are acceptable.

Table 9: Bearings Dynamic Forces and Rotor Displacements

Parameter	Direction	Baseline		Optimized	
		DE	NDE	DE	NDE
Unbalance case 1					
Dynamic Force, N	Horizontal	2291	1739	1294	864
	Vertical	3216	2746	2105	1663
Major displacement, peak-to-peak µm	Absolute	31	29	21	17
	Housings	8.9	6.5	4.7	3.1
	Supports	7.5	4.8	3.9	2.2
	Relative	22.1	22.5	16.3	13.9
Unbalance case 2					
Dynamic Force, N	Horizontal	1286	1325	1661	1727
	Vertical	1972	2020	2678	2841
Major displacement, peak-to-peak, µm	Absolute	17	21	27	33
	Housings	4.8	4.7	5.8	5.7
	Supports	4	3.5	4.9	4.2
	Relative	12.2	16.3	21.2	27.3

Logarithmic decrement plot was generated to check the optimized rotor-bearing system stability and presented in Fig. 14. The logarithmic decrement values for considered mode (corresponding 1st, 2nd, and 3rd critical speeds) are higher than 0.1 and show stable behavior for the design.

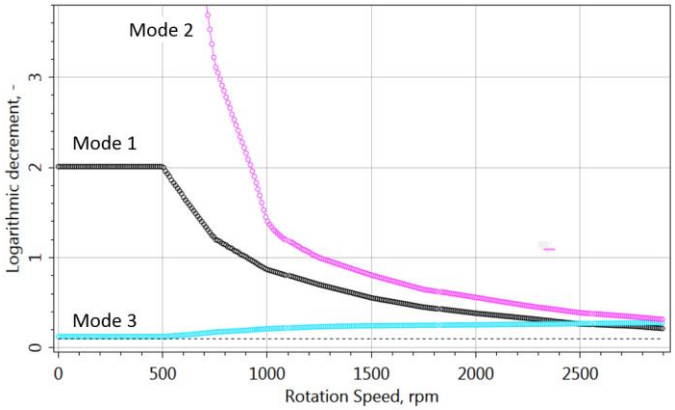

Figure 14: Logarithmic decrement calculated for the optimized rotor-bearing system

CONCLUSION

The approach, which allows to improve bearings characteristics and change critical speeds for the rotor-bearing system to avoid potential resonances was developed.

The methodology was applied to 13.5 MW induction motor rotor-bearing system. Three different bearing types were considered for the application to find the optimal design for the system. Optimal parameters for the rotor-bearing system were generated and following goals of optimization were solved:

1) Critical speeds margins for the rotor-bearing system according to API standards have been met;
2) Friction loss was minimized for the bearing designs;
3) The acceptable level of the minimal oil film thickness has been provided.

It should be noted that considered optimization objectives are contradictory, to be exact, the maximum minimal oil film thickness does not yield a low power loss or good rotor dynamics behavior for the rotor-bearing system. For that reason, optimized functions don't have absolute optimal values (maximal or minimal), but the design can be considered optimal in total.

High accuracy of the applied optimization with macromodels have been confirmed by comparison with the data simulated in Bearing and RotorDynamics solvers. Another advantage of the approach is that all simulations are done within an integrated system, which automates and accelerate the optimization process.

The proposed method is recommended to be applied to many industrial applications (turbines, compressors, fans, pumps, and etc.) at the design phase to optimize rotor-bearing system performance characteristics and provide a minimal level of vibrations.

REFERENCES

[1] Sutariya C., Tamboli K., George P.M., 2011, "Optimum Design of A Journal Bearing – A Review", National Conference on Recent Trends in Engineering & Technology, India.

[2] Weißbacher, C., 2014, "Optimization of Journal Bearing Profiles With Respect to Stiffness and Load-Carrying Capacity", Wiley-Verlag, New York, USA.

[3] Hirania H., Suhb N.P., 2004, "Journal bearing design using a multiobjective genetic algorithm and axiomatic design approaches", Tribology International, United Kingdom.

[4] Saruhan H., Rouch K.E., Roso C.A, 2002 "Design Optimization of Tilting-Pad Journal Bearing using a Genetic Algorithm", International Journal of rotating machinery, London, United Kingdom.

[5] Amit S., Prakash P., Bhargirath P., 2014, "Design Formulation and Optimum Load Carrying Capacity of Hydrodynamic Journal Bearing By using Genetic Algorithm", International Journal for research in applied science and engineering technology, Faridabad, India.

[6] Havlik N., Lutz M., 2015, "Optimization of tilting-pad journal bearings for integrally geared compressors", ASME Turbo Expo, Montreal, Canada.

[7] Cao J., Dimond T., 2015, "Reduction of vibration and power loss in industrial turbochargers with improved tilting pad bearing design", ASME Turbo Expo, Montreal, Canada.

[8] Biswas N., Chakraborti P., Dhar P., 2016, "Optimization of pressure and oil film thickness in Multilobe Bearing using Response Surface Methodology and Moga", Journal of Scientific & Industrial Research, Vol. 75 (08).

[9] API, 684, 2005. *API recommended practice*, American petroleum institute, Washington, USA.

[10] Untaroiu C.D., Untaroiu A., 2010, "Constrained Design Optimization of Rotor-Tilting Pad Bearing Systems", J. Eng. Gas Turbines Power 132(12)

[11] Box E. P., D.W. Benken, "Some new three-level design for the study of quantitative variables", Technometrics, 1967, 2(4).
[12] Sobol I.M., Statnikov R.B., 2006, *Optimal parameters selection for the tasks with multiple criteria.* Drofa, Moscow, Russia.
[13] Elrod, H.G., Adams, M., 1974, “A computer program for cavitation and starvation problems. Technical report 190.” 1st LEEDS LYON Symposium on Cavitation and Related Phenomena in Lubrication, I.M.E., 103, pp. 37–41.
[14] API 541, Fifth Edition, 2014. *Form-wound Squirrel Cage Induction Motors-375 kW (500 Horsepower) and Larger*, American petroleum institute, Washington, USA.
[15] API 546, Third Edition, 2008. *Brushless Synchronous Machines - 500 kVA and Larger*, American Petroleum Institute, Washington, USA.
[16] Neto, R.R., Bogh, D.S., and Flammia, M., 2008, ”Some Experiences on Rigid and Flexible Rotors in Induction Motors Driving Critical Equipment in Petroleum and Chemical Plants”, IEEE Transactions on Industry Applications.